Received: Added at production | Revised: Added at production | Accepted: Added at production

DOI: xxx/xxxx

RESEARCH ARTICLE

Hemispheric Complementarity in Hippocampal Theta Dynamics during Mnemonic Decision-Making

Pei L. Robins[1] | Jessica R. Gilbert[1] | Bruce Luber[1] | Nadia Mustafa[1] | Eesha Bharti[1] | Jeffrey D. Stout[2] | Frederick W. Carver[2] | Zhi-De Deng[1]

[1]Experimental Therapeutics and Pathophysiology Branch, National Institute of Mental Health, National Institutes of Health, Bethesda, MD, USA

[2]Magnetoencephalography Core Facility, National Institute of Mental Health, National Institutes of Health, Bethesda, MD, USA

Correspondence
Zhi-De Deng (zhi-de.deng@nih.gov)

Present address
10 Center Drive, Bethesda, MD 20892, USA

Funding Information
This research was supported by the National Institute of Mental Health (NIMH) Intramural Research Program (ZIAMH002927 and ZIAMH002955).

Abstract

A core function of episodic memory is to distinguish between overlapping experiences by converting similar inputs into distinct, non-overlapping representations—a process termed pattern separation. While anatomical models emphasize the role of specific hippocampal subfields, particularly the dentate gyrus, CA3, and CA1, less is known about how these computations unfold over time and influence memory-based decisions. Here, we use source-localized magnetoencephalography and computational modeling to examine how theta oscillations from the hippocampus as a whole are related to evidence accumulation during mnemonic discrimination. Participants performed the Mnemonic Similarity Task, in which they classified repeat, lure, and foil images as "old," "similar," or "new." We fit a hierarchical Linear Ballistic Accumulator model to behavioral data, estimating trial-by-trial drift rates—a latent index of mnemonic evidence accumulation—and examined whether hippocampal theta power predicted these dynamics. Theta power in the left hippocampus was positively associated with drift toward "new" responses across stimulus conditions, consistent with a novelty-oriented decision bias. In contrast, right hippocampal theta showed negative associations with drift toward familiarity-driven false alarms to foil items, suggesting a complementary mechanism that curtails evidence accumulation based on false familiarity. Both hemispheres showed positive theta–drift associations during correct "similar" responses, implicating bilateral coordination in successful discrimination. Event-related source activity confirmed reliable hippocampal engagement despite the anatomical depth of the source. These findings reveal a dynamic, lateralized mechanism by which hippocampal theta oscillations shape memory-guided decisions, offering new insight into how the brain resolves mnemonic uncertainty in real time.

KEYWORDS
Pattern separation, mnemonic similarity task, hippocampus, theta oscillations, magnetoencephalography, linear ballistic model

1 | INTRODUCTION

Episodic memory enables the recollection of specific past experiences not only by preserving their content, but also by differentiating among events that overlap in time, space, or perceptual detail (Eichenbaum, 2017, Tulving, 1983). This ability to disambiguate similar experiences is thought to rely on a process known as pattern separation, in which inputs—such as events that share temporal, spatial, or perceptual features—are transformed into orthogonalized neural representations to minimize interference (O'Reilly & McClelland, 1994, Yassa & Stark, 2011). The transformation is implemented through complementary mechanisms within the hippocampal circuit, in particular, the dentate gyrus (DG), and the CA3 and CA1 subfields. The DG provides sparse, non-overlapping representations of cortical inputs through low activation rates and random connectivity patterns, which decorrelate incoming signals (Leutgeb et al., 2007, Rolls, 2013, Treves & Rolls, 1994, Yassa & Stark, 2011). In contrast, the CA3 subfield, with its dense recurrent collaterals, supports autoassociative storage and pattern completion by enabling retrieval from partial cues. CA3 can also contribute to pattern separation under conditions of sufficiently distinct input or strong DG drive, exhibiting flexible dynamics depending on input similarity (Leutgeb et al., 2007, Yassa & Stark, 2011). Recent physiological work further supports this computational architecture: Allegra et al. demonstrated

 © 2025 Copyright Holder Name

that while the DG consistently decorrelates similar inputs regardless of behavioral outcome, CA1 selectively reflects behaviorally relevant distinctions, suggesting that downstream hippocampal regions gate and interpret the output of DG–CA3 computations according to task demands (Allegra et al., 2020). These complementary properties allow the DG–CA3–CA1 circuit to flexibly support both memory discrimination and generalization. Increasingly, research suggests that this balance is not only anatomically distributed but also temporally orchestrated. In particular, hippocampal theta oscillations (4–8 Hz) have emerged as a dynamic scaffold for coordinating encoding and retrieval processes.

These oscillations organize neural activity into alternating phases that bias the hippocampus toward either external input or internal retrieval: during one phase of the theta cycle, entorhinal input dominates, supporting pattern separation and encoding; during the opposite phase, CA3 input prevails, promoting pattern completion and retrieval (Colgin, 2013, Hasselmo et al., 2002). This functional segregation minimizes interference between incoming and stored information. Moreover, evidence from intracranial electroencephalography (iEEG) confirms that increased theta power preceding stimulus onset predicts later memory success, highlighting theta's role in establishing a preparatory mnemonic state (Fell et al., 2011, Guderian et al., 2009). Buzsáki further conceptualizes theta as a temporal organizer of hippocampal assemblies, aligning neuronal firing with windows of synaptic plasticity (Buzsáki, 2002). Theta's role extends to retrieval: phase synchrony between the hippocampus and neocortex facilitates the reinstatement of previously encoded representations (Osipova et al., 2006). In behavioral contexts requiring memory-guided decisions, theta rhythm helps resolve competition among overlapping traces by structuring neural computation into discrete, state-specific epochs (Hasselmo, 2005, Herweg et al., 2020). Despite this compelling framework, much of the empirical literature relies on trial-averaged estimates of theta power, leaving open how trial-level fluctuations in hippocampal theta contribute to memory performance and decision-making in contexts demanding mnemonic discrimination. To bridge this gap, behavioral paradigms are needed that both elicit fine-grained mnemonic discrimination and can be aligned with temporally resolved neural dynamics.

The Mnemonic Similarity Task (MST) provides a robust and well-validated tool for studying the neural mechanisms of mnemonic discrimination (Stark et al., 2019). The task consists of two phases: during encoding, participants view a series of images depicting common everyday objects; during retrieval, they are asked to classify each item as "old," "similar," or "new" from a mixed set that includes repeated items, similar but non-identical lures, and novel items. Crucially, accurate identification of lures as "similar" is interpreted as behavioral evidence of pattern separation, while misclassification of lures as "old" is often taken to reflect pattern completion or memory generalization. This interpretive framework maps onto the proposed computational architecture of the hippocampus described above: activity in the DG is thought to support successful lure discrimination, whereas the CA3 subfield modulates the tradeoff between separation and completion based on input similarity (Bakker et al., 2008, Berron et al., 2016, Yassa et al., 2011). Functional magnetic resonance imaging (fMRI) studies have consistently implicated DG/CA3 activity in lure discrimination, yet the slow temporal resolution of fMRI limits access to the rapid computations that shape memory decisions. Moreover, MST decisions are inherently ambiguous: lures are designed to resemble repeats, and accurate responding requires resolving this perceptual and mnemonic overlap in real time. For this reason, the MST offers a valuable context not only for probing hippocampal function but also for examining how memory signals are transformed into decisions under uncertainty. However, the task's behavioral outcome—response time (RT)—reflects the aggregate duration of multiple cognitive processes, including visual processing, evidence accumulation, and motor execution (button press). As a result, it is difficult to isolate specific decision-related computations. To access the quality and dynamics of mnemonic evidence more directly, computational modeling is required.

Sequential sampling models such as the Linear Ballistic Accumulator (LBA) offer a principled framework for disentangling the cognitive processes underlying memory-based decisions (Brown & Heathcote, 2008, Donkin et al., 2011). The model decomposes observed choices and RTs into latent parameters, among which *drift rate* quantifies the quality and speed of evidence accumulation. This parameter is particularly well-suited to capture trial-level variability in mnemonic strength, especially in tasks like the MST that demand fine-grained discrimination under uncertainty. Demonstrating this application, Banavar et al. applied the LBA to MST performance and identified drift rate as a meaningful and interpretable marker of mnemonic evidence strength (Banavar et al., 2024). Electrophysiological correlates have been observed, as studies have demonstrated that both event-related potentials and oscillatory dynamics track continuous variation in decision evidence—across both perceptual and mnemonic domains—and correlate with model-derived measures of decision processing (Addante et al., 2011, Philiastides & Sajda, 2006, Ratcliff et al., 2009). In parallel, neuroimaging studies have identified drift rate correlates in parietal and prefrontal cortices during memory-based decisions (Mueller et al., 2017, Mulder et al., 2014), reinforcing the broader utility of these models for linking cognitive computations to brain activity.

Despite these advances, no studies to date have directly linked measures of single-trial neural dynamics, such as hippocampal theta oscillations, to computational parameters of decision-making during mnemonic discrimination. This lack of integration leaves a critical gap in our understanding: while computational models offer mechanistic insight into behavior, and neural signals reflect ongoing cognitive processing, the two have yet to be combined at the level of individual memory decisions. Bridging this divide is essential for connecting cognitive theory to neural mechanisms in a temporally precise and functionally interpretable manner.

In the present study, we address this gap by combining source-localized magnetoencephalography (MEG) with LBA modeling during the MST. Our primary aim was to determine whether trial-by-trial fluctuations in hippocampal theta power predict the rate of evidence accumulation during memory decisions, and whether these relationships

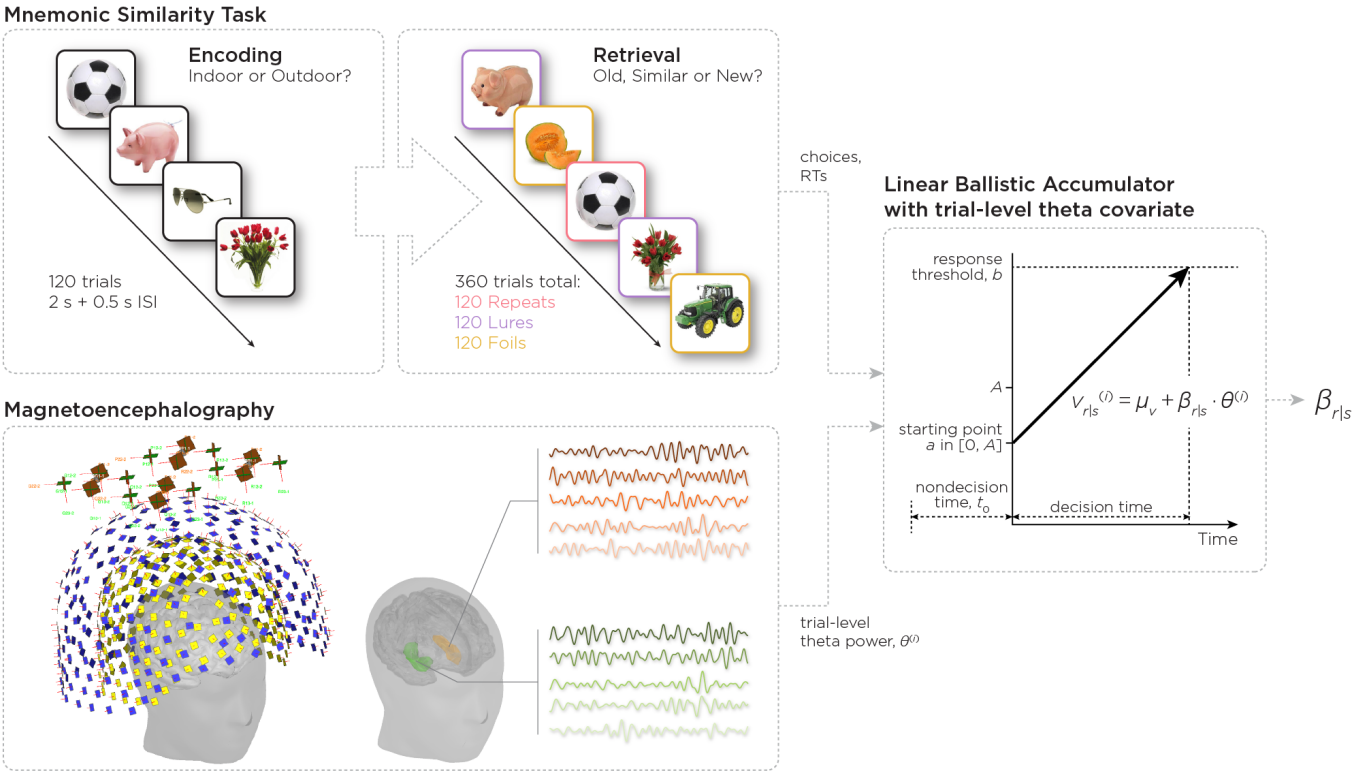

FIGURE 1 Overview of experimental design and modeling approach. Participants performed a two-phase Mnemonic Similarity Task during magnetoencephalography. During the encoding phase (top left), participants viewed 120 images of everyday objects and made "indoor"/"outdoor" judgments. In the retrieval phase, they classified 360 objects as "old," "similar," or "new," corresponding to repeats, lures, and foils, respectively. Magnetoencephalography signals were recorded continuously (bottom left), and hippocampal time series were reconstructed using source localization techniques. Trial-level theta-band power (4–8 Hz) was extracted separately for the left and right hippocampus to measure retrieval-related neural activity. These theta estimates were then entered as covariates in a hierarchical Linear Ballistic Accumulator model (right), which decomposed choice and response time (RT) data into latent decision parameters. Drift rate was modeled as a linear function of theta power, and the regression coefficient $\beta_{r|s}$ quantifies how trial-level theta power relates to variation in evidence accumulation across trials for that specific stimulus–response pairing.

differ across hemispheres. Although the hippocampus has been widely implicated in pattern separation, many prior studies have either pooled across hemispheres, focused on long-axis (anterior–posterior) gradients, or examined subfield-level effects without reporting lateralization. Yet several lines of research suggest that the left and right hemispheres may support distinct contributions to memory. For example, the Hemispheric Encoding/Retrieval Asymmetry (HERA) model (Tulving et al., 1994) proposed a functional division between left-lateralized encoding and right-lateralized retrieval processes in episodic memory. While HERA emphasized prefrontal contributions, more recent studies point to anatomical, functional, and oscillatory asymmetries across the left and right hippocampus, suggesting that lateralized dynamics may extend beyond the cortex (Penner et al., 2022, Stevenson et al., 2020). Building on this literature, our MEG source modeling approach allowed us to estimate hippocampal activity separately in each hemisphere and to study lateralization in theta-related decision dynamics. Prior MEG work has demonstrated that hippocampal responses can be detected under recognition memory conditions when appropriate source modeling techniques are used, including beamforming and spectral analyses in the theta band (Riggs et al., 2009). By linking oscillatory neural dynamics directly to computational indices of decision-making, our approach offers a novel framework for identifying the mechanistic role of hippocampal theta in evidence accumulation. In doing so, it advances the integration of cognitive and neural accounts of pattern separation in human episodic memory.

2 | METHODS

2.1 | Participants

Twenty healthy volunteers were initially enrolled in the study, which was conducted under a National Institutes of Health (NIH) technical development protocol aimed at advancing neuroimaging methods for studying mood and anxiety disorders (ClinicalTrials.gov ID:

NCT00397111). Five participants were excluded from the analysis due to missing structural magnetic resonance imaging (MRI) scans ($n = 3$) or poor behavioral task performance ($n = 2$), the latter due to drowsiness or misunderstanding task instructions. The final sample consisted of fifteen participants (14 female, 1 male), with a mean age of 31 years (range: 21–54). All participants were right-handed, reported normal or corrected-to-normal vision, and had no history of neurological or psychiatric disorders. Written informed consent was obtained from all participants, and all procedures were approved by the Institutional Review Board of the National Institute of Mental Health (NIMH).

2.2 | Behavioral Task

Participants performed the Mnemonic Similarity Task (MST) (Stark et al., 2019) while seated in the magnetoencephalography (MEG) scanner (MEG Core Facility, NIH). The task, designed specifically to probe hippocampal pattern separation, comprised an encoding phase and a retrieval phase, implemented using PsychoPy2 (Peirce et al., 2019). During the encoding phase, participants viewed 120 images of everyday objects, making "indoor"/"outdoor" judgments for each item. During the retrieval phase, participants classified 360 images as "old," "similar," or "new." These images included 120 previously viewed items (repeats), 120 similar but non-identical items (lures), and 120 novel items (foils). All stimuli were presented for 2 seconds, followed by a 0.5-second interstimulus interval between the subsequent trials (Figure 1).

2.3 | Behavioral Indices: Lure Discrimination Index and Recognition Score

To quantify memory performance during the MST, we computed two behavioral indices: the *Lure Discrimination Index (LDI)* and the *Recognition Score (REC)*. The LDI reflects the ability to distinguish similar lures from novel foils, adjusted for response bias, and is defined as:

$$\text{LDI} = \text{P}(\text{response} = \text{“Similar”} \mid \text{stimulus} = \text{Lure}) - \text{P}(\text{“Similar”} \mid \text{Foil}). \tag{1}$$

The Recognition Score (REC) reflects corrected recognition memory by adjusting for false alarms to novel stimuli. It is defined as:

$$\text{REC} = \text{P}(\text{“Old”} \mid \text{Repeat}) - \text{P}(\text{“Old”} \mid \text{Foil}). \tag{2}$$

These definitions follow prior work characterizing behavioral performance in the MST (Stark et al., 2019).

2.4 | Imaging Data Acquisition and Preprocessing

Structural MRI scans were acquired using a 3T GE (General Electric) gradient-echo scanner equipped with a 32-channel head coil. A high-resolution T1-weighted MP-RAGE sequence was used to obtain anatomical images for source modeling [field of view = 256 mm^2; voxel size = 1 mm isotropic; echo time (TE) = minimum full; inversion time (TI) = 1100 ms; flip angle = 7°; bandwidth = 25 Hz/pixel].

To measure neural activity during the task, we recorded MEG data using a whole-head CTF MEG system (CTF Systems, Inc., Canada), which includes 275 radial first-order gradiometer SQUID channels. Head position was continuously monitored using three localization coils placed at fiducial landmarks. These coils were positioned 1.5 cm above the nasion, and at left and right preauricular points (1.5 cm anterior to each tragus along a line extending through the outer canthus of the eye). Fiducial locations were co-registered to each participant's MRI using Brainstorm (Tadel et al., 2011). Data were acquired continuously with an online synthetic third-order gradiometer configuration to suppress environmental magnetic interference. Data were primarily sampled at 600 Hz with an acquisition bandwidth of 0–150 Hz. Due to variability in hardware settings, recordings of three participants were sampled at 1200 Hz.

Following the acquisition, all data analysis was performed in Brainstorm. Data sampled at 1200 Hz were downsampled to 600 Hz, and all data were bandpass filtered between 1 and 100 Hz. A 60 Hz notch filter was applied to suppress line noise. Artifact correction was performed on the continuous data using Infomax independent component analysis (ICA) to identify and remove components associated with ocular, cardiac, and muscle artifacts. Components were manually evaluated using a combination of time course, topography, and frequency characteristics. Following ICA, the data were segmented into epochs ranging from 200 ms before to 1000 ms after stimulus onset, and trials containing residual high-amplitude transients were excluded from further analysis. Trials with response times (RTs) less than 200 ms or no response were also excluded from the analysis, as such responses are unlikely to reflect genuine stimulus-driven decisions.

2.5 | Source Modeling and Event-Related Signal Extraction

Individualized head models were computed using the overlapping spheres method implemented, and source estimation was performed using a depth-weighted dynamic statistical parametric mapping (dSPM) approach (Dale et al., 2000). Dipole orientations were constrained normal to the cortical and hippocampal surfaces (Attal et al., 2009, Attal & Schwartz, 2013), as defined by anatomical parcellation from FreeSurfer 7.4.1 Automatic Subcortical Segmentation (ASEG) atlas (Fischl, 2013).

Source time series were extracted from dSPM values within left and right hippocampal regions of interest (ROIs). To account for ambiguity in dipole polarity and to derive a representative signal per hemisphere, we computed the root-mean-square (RMS) across all dipoles within each ROI. These RMS time series were baseline-corrected using a 200-ms pre-stimulus window and transformed into *Z*-scores, yielding standardized, stimulus-locked estimates of hippocampal activity.

To verify that hippocampal sources exhibited task-evoked responses with sufficient signal-to-noise ratios, we computed event-related fields (ERFs) by averaging the source-localized RMS time series across trials for each task phase and condition. Visual inspection of group-averaged ERFs focused on response magnitude, latency, and temporal dynamics, confirming robust and temporally consistent hippocampal activation in response to MST stimuli.

2.6 | Single-Trial Theta Power Estimation

To quantify trial-by-trial fluctuations in hippocampal oscillatory activity, we estimated theta-band (4–8 Hz) power from source-localized time series in the left and right hippocampus. Each dSPM time series was bandpass filtered using a zero-phase finite impulse response filter, and the analytic signal was computed via the Hilbert transform. Instantaneous power was obtained by squaring the magnitude of the resulting complex signal and averaged over the 1000-ms post-stimulus window. Power values were then normalized relative to the 200-ms pre-stimulus baseline, providing baseline-corrected estimates of stimulus-evoked theta activity on a trial-by-trial basis.

2.7 | Linear Ballistic Accumulator Modeling with Theta Power Covariate

To model latent decision dynamics during the MST, we implemented a hierarchical Bayesian Linear Ballistic Accumulator (LBA) model using RStan (Stan Development Team, 2024). The LBA characterizes decision-making as a race among linear accumulating evidence streams—one for each response alternative. On each trial, the first accumulator to reach its threshold determines both the choice and RT. In our case, each trial involved three independent accumulators corresponding to the response types: "old," "similar," and "new."

We estimated drift rates for each combination of stimulus condition (repeat, lure, foil) and response type, yielding a 3×3 matrix of drift parameters ($v_{r|s}$), where r indexes response and s stimulus. Other latent parameters included the starting point a, decision threshold b, and non-decision time t_0, as well as between-trial variability in drift (σ_v) and starting point (σ_a). These were modeled hierarchically, allowing for subject-level deviations from group-level means. A total of 5,262 trials were included in the model, with all 15 participants contributing data (mean = 351 trials per participant, range = 314–359).

To examine whether trial-by-trial fluctuations in hippocampal theta power predicted variability in drift rate, we extended the standard model by incorporating single-trial theta power as a covariate. This was achieved by modeling drift as a linear function of theta power:

$$v_{r|s}^{(i)} = \mu_{v_{r|s}} + \beta_{r|s} \cdot \theta^{(i)}, \tag{3}$$

where $v_{r|s}^{(i)}$ is the drift rate on trial i for response r given stimulus s, $\mu_{v_{r|s}}$ is the group-level mean drift rate, $\beta_{r|s}$ is the regression coefficient capturing the effect of theta power on drift, and $\theta^{(i)}$ is the theta power from either the left or right hippocampus. Separate models were fit for each hemisphere to isolate lateralized effects.

Initial values were defined to ensure identifiability, with start points a constrained to lie below thresholds b. Group-level means (μ_v, μ_a, μ_b, μ_{t_0}) and standard deviations (σ_v, σ_a, σ_b, σ_{t_0}) were given weakly informative priors centered around canonical values used in the literature. However, unlike some previous implementations (e.g., (Banavar et al., 2024)), we did not impose a simplex constraint on the drift rates across response types, i.e., $\sum_{r=1}^{3} v_r = 1$. The sum-to-one constraint normalizes drift rates across accumulators and thus enforces a competitive allocation of evidence. While this may enhance interpretability in studies comparing static choice preferences, it introduces dependencies among parameters that can obscure independent modulations by neural predictors. Because our primary aim was to assess how theta power relates to the absolute quality and speed of evidence accumulation across different decision types, we allowed drift rates and starting points to vary independently across stimulus–response pairings. This approach accommodates the possibility that theta-related effects increase or decrease accumulation globally, rather than simply reallocating it among alternatives.

Model fitting was performed using Hamiltonian Monte Carlo (HMC) sampling via the No-U-Turn Sampler (NUTS) (Carpenter et al., 2017). Four independent chains were run, each with 10,000 iterations, including 2,000 warm-up iterations, resulting in 32,000 post-warmup samples for posterior inference. Convergence was assessed using potential scale reduction factors ($\hat{R}$), effective sample sizes, and visual inspection of trace plots (Vehtari et al., 2021). Posterior distributions of the $\beta_{r|s}$ coefficients were used to assess the influence of hippocampal theta power on drift rates for each stimulus–response pairing. 95% credible intervals were computed from the posterior distributions, and inference focused on whether these intervals excluded zero (no theta effect).

3 | RESULTS

3.1 | Behavioral Performance and Drift Rate Estimates

To quantify behavioral performance during the Mnemonic Similarity Task (MST), we computed two accuracy-based indices that separately captured recognition and discrimination. The mean Recognition Score (REC) was 0.57, indicating a moderate ability to distinguish previously seen items from novel foils. The mean Lure Discrimination Index (LDI) was 0.33, consistent with normative values observed in large samples of healthy adults (Banavar et al., 2024).

Next, we examined the proportion of responses (Figure 2A) and the mean response times (RTs) across stimulus–response combinations

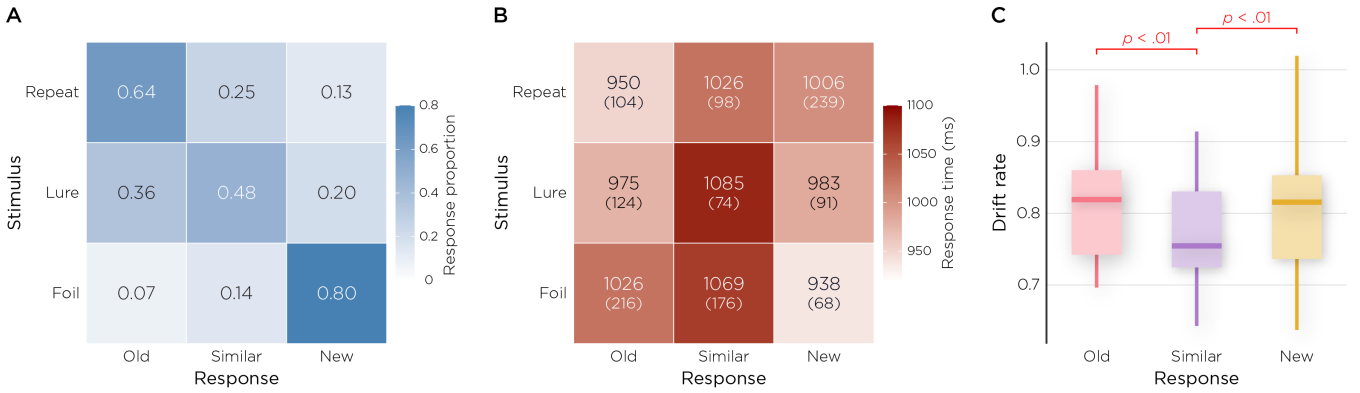

FIGURE 2 Behavioral performance and model-derived drift rates in the Mnemonic Similarity Task. (A) Proportion of responses across all combinations of stimulus condition (repeat, lure, foil) and response type ("old", "similar", "new"), averaged across participants. (B) Median response times (in ms) were computed for each participant and then averaged across the group for each stimulus–response pairing. Parentheses indicate standard deviations across participants. (C) Mean drift rate estimates from the Linear Ballistic Accumulator model, grouped by response type. Drift rates were significantly lower for "similar" responses than for "old" or "new" responses ($p < .01$).

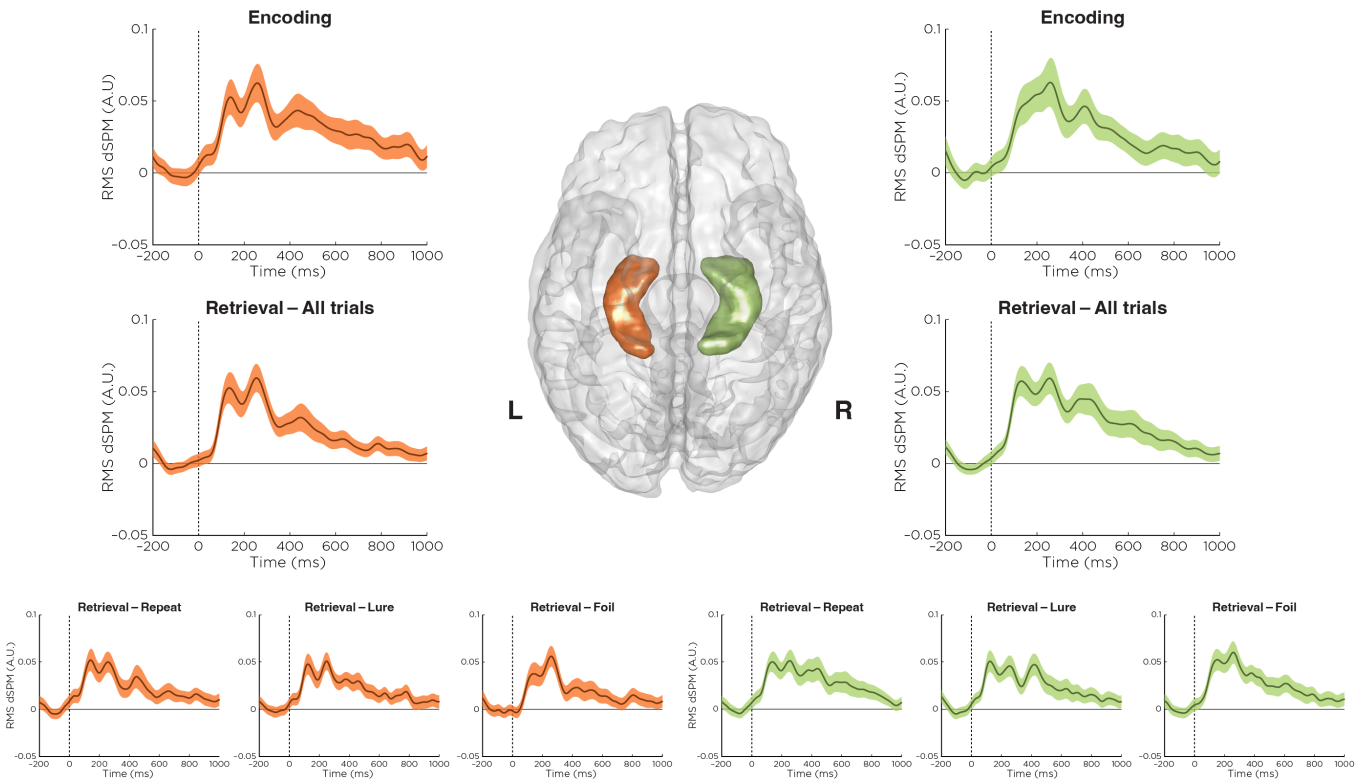

FIGURE 3 Average source-localized time series were extracted from left (orange) and right (green) hippocampi, computed as root-mean-square (RMS) of dynamic statistical parametric mapping (dSPM) *Z*-score values, and baseline-corrected using a 200-ms pre-stimulus window. Top row: Event-related fields (ERFs) during the encoding phase of the Mnemonic Similarity Task; Middle row: ERFs during the retrieval phase, averaged across all stimulus types; Bottom row: Retrieval-phase ERFs separated by stimulus type (repeats, lures, foils). Although dSPM values are shown in arbitrary units (A.U.) due to *Z*-scoring prior to averaging, stimulus-evoked responses were observed in both hemispheres. Narrow standard error bands indicate high consistency across participants.

(Figure 2B). Trials in which participants responded "similar" were generally observed with longer RTs than "old" or "new" responses, consistent with the increased difficulty of correctly rejecting lures. However, because RTs reflect the aggregate of multiple cognitive operations, they

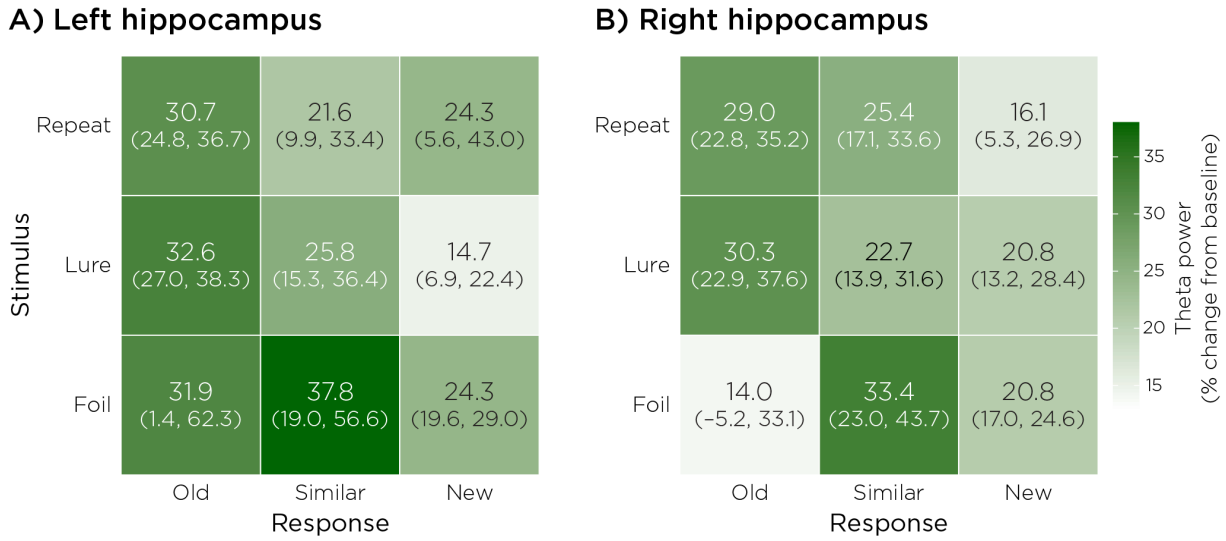

FIGURE 4 Mean theta power (4–8 Hz) in the hippocampus across stimulus–response pairings. Each cell represents the group-averaged theta power (expressed as percent change from pre-stimulus baseline). Parentheses denote 95% bootstrap confidence intervals across participants. Theta power was elevated above baseline in nearly all conditions, indicating that hippocampal theta engagement is a general feature of retrieval-phase processing during the Mnemonic Similarity Task.

offer limited specificity about the decision process itself. To more directly infer the quality and dynamics of mnemonic evidence, we applied the Linear Ballistic Accumulator (LBA) model to estimate the underlying rate of evidence accumulation for each response type. Posterior sampling showed good convergence for all critical parameters ($\hat{R} \leq 1.003$), with high effective sample sizes and well-mixed chains. As shown in Figure 2C, drift rates were significantly slower for "similar" responses than for "old" or "new" responses ($p < .01$), reflecting slower and more variable evidence accumulation in trials requiring fine mnemonic discrimination.

3.2 | Hippocampal Event-Related Fields and Theta Power

To establish whether hippocampal sources were reliably engaged during the task, we examined event-related fields (ERFs) derived from source-localized time series (Figure 3). Stimulus-locked responses were evident in both hemispheres. Across both task phases, the group-averaged time courses revealed a well-defined response starting at approximately 100 ms after stimulus onset, followed by a polyphasic wave peaking between 200–300 ms, and a smaller subsequent peak between 400–500 ms. Importantly, the narrow standard error bands indicated consistent temporal dynamics across participants. Retrieval-phase responses were broadly similar across stimulus conditions (repeat, lure, foil), with no strong qualitative differences between the left and right hippocampi. Together, these results demonstrate reliable stimulus-evoked hippocampal activity and provide a foundation for analyzing trial-level theta fluctuations in relation to memory-based decision-making.

As shown in Figure 4, theta power was elevated relative to baseline in nearly all conditions, with the strongest increases in the left hemisphere for "old" responses. Bootstrap confidence intervals confirmed that these effects were robust across participants.

3.3 | Theta-Dependent Drift Rates

We next asked whether trial-by-trial fluctuations in hippocampal theta power predicted variability in evidence accumulation. To test this, we incorporated single-trial theta power estimates into the LBA model as predictors of drift rate, separately for the left and right hippocampus. Figure 5 shows the resulting regression coefficients (β), representing the effect of theta power on drift rate across all combinations of stimulus and response. In the left hippocampus (Figure 5A), theta power was positively associated with drift rates for "new" responses regardless of the stimulus type. In contrast, the right hippocampus (Figure 5B) showed negative associations between theta power and drift rates for incorrect "similar" and "old" responses to novel foil items. Both hemispheres showed a significant positive association between theta power and drift rate for correct "similar" responses to lures.

4 | DISCUSSION

The present study builds on recent efforts to model memory-based decisions using formal evidence accumulation frameworks. In particular, Banavar et al. (Banavar et al., 2024) applied the Linear Ballistic Accumulator (LBA) model to the Mnemonic Similarity Task (MST), demonstrating that drift rate—a parameter indexing the quality and

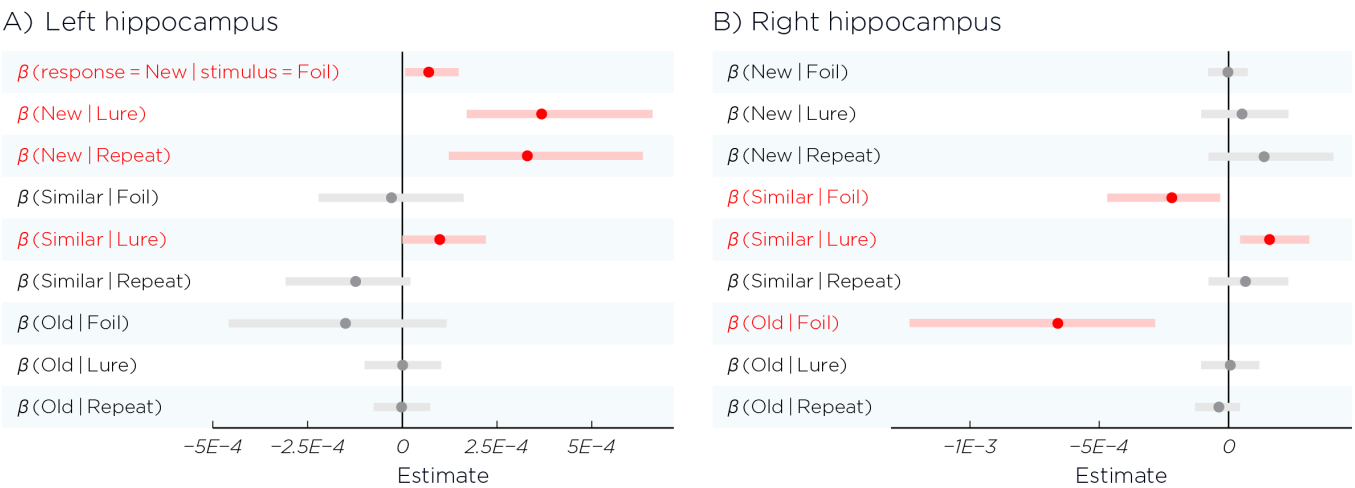

FIGURE 5 Effects of single-trial hippocampal theta power on drift rate during mnemonic decisions. Posterior estimates of β coefficients from the Bayesian Linear Ballistic Accumulator, modeling drift rate as a function of trial-level theta power, separately for the left (A) and right (B) hippocampus. Each β coefficient reflects the effect of theta power on the drift rate for a given response type, conditioned on the stimulus type, e.g., β(Similar|Lure), indicates the influence of theta power on evidence accumulation for a "similar" response to a lure stimulus. Error bars represent 95% credible intervals. Red markers indicate statistically significant effects ($p < .05$), and gray markers indicate non-significant effects. In the left hippocampus, theta power was positively associated with drift rates for "new" responses regardless of the stimulus type [β(New|Foil), β(New|Lure), and β(New|Repeat)], suggesting a response bias toward novelty. In contrast, right hippocampal theta was associated with a suppression of such bias, showing negative associations with drift rates for *incorrect* "similar" and "old" responses to novel foil items [β(Similar|Foil) and β(Old|Foil)]. Importantly, both hemispheres showed a significant positive association between theta power and drift rate for correct "similar" responses to lures [β(Similar|Lure)], indicating a bilateral role of hippocampal theta in successful mnemonic discrimination.

speed of evidence accumulation—offers a mechanistically interpretable alternative to surface-level behavioral metrics such as response time (RT) and accuracy (also see Supplementary Analysis). Consistent with their findings, we observed that drift rates were significantly lower for "similar" responses than for "old" or "new" responses, suggesting that lure discrimination decisions are based on weaker or more ambiguous mnemonic evidence. These results reinforce the interpretation that drift rate reflects the strength of internal memory signals rather than general response bias or threshold adjustment. Extending this framework, we next asked whether hippocampal theta power—a well-established neural correlate of episodic memory—predicts the dynamics of evidence accumulation during individual mnemonic decisions.

While hippocampal theta power was broadly elevated across nearly all stimulus–response conditions during the retrieval phase of the MST, this global increase alone does not account for the observed variation in behavioral performance. Average-level effects, though indicative of general retrieval-related engagement, obscure the functional specificity of theta activity in shaping decisions. A similar pattern has been observed in prior magnetoencephalography (MEG) studies. For example, Riggs et al. used Synthetic Aperture Magnetometry to examine theta power during complex scene recognition and found no significant differences between old and new stimuli, suggesting that hippocampal theta may reflect a general recognition-related process rather than selective responses to novelty or familiarity (Riggs et al., 2009). To move beyond average effects, we modeled trial-specific theta power and tested whether it predicted drift rates across conditions. This analysis revealed that, even against the backdrop of elevated theta, only a subset of stimulus–response pairings showed reliable theta–drift relationships—indicating that it is not merely the presence of theta, but its moment-to-moment fluctuations, that track the dynamic cognitive processes underlying memory-based decisions. This predictive specificity aligns with recent physiological evidence that theta in the human hippocampus occurs in sparse, intermittent bursts rather than as continuous oscillations, even during memory tasks (Penner et al., 2022), reinforcing the importance of trial-level analyses in uncovering the functional role of theta dynamics.

A central finding of the present study was a striking hemispheric complementarity in the relationship between hippocampal theta power and the rate of evidence accumulation across memory decisions. In the left hippocampus, trial-by-trial increases in theta power were associated with increased drift rates toward "new" responses across all stimulus conditions, indicating a general novelty response bias. However, this reflects more than just novelty detection, but a novelty-driven discrimination. Note that the association was strongest when presented with lures and repeats [β(New | Lure), β(New | Repeat)]—stimuli that share mnemonic overlap with previously seen items—suggesting that theta-related novelty signals are most influential when disambiguating between similar memory traces. The weaker association for foils [β(New | Foil)], which are entirely novel and lack mnemonic interference, implies that less hippocampal theta engagement is needed

when novelty is unambiguous. In the right hippocampus, higher trial-by-trial theta power was associated with reduced drift rates for false alarms, specifically, "similar" and "old" responses to foil stimuli. This pattern suggests that theta activity may play a role in suppressing unwarranted familiarity signals or restricting the intrusion of inappropriate memory-based evidence when novelty should be detected. Rather than promoting a specific decision outcome, the right hippocampus appears to constrain or gate evidence accumulation when the stimulus does not warrant a memory response. Taken together, these lateralized effects suggest a functional asymmetry in how hippocampal theta activity supports mnemonic decisions. Although these effects are computationally opposing—left enhancing versus right suppressing drift rates—they are functionally complementary: the left pushing accumulation toward novelty when ambiguity is high and the right pulling back when familiarity is misleading.

Hemispheric asymmetries in the human hippocampus are well documented. The left hippocampus has been linked to semantic and associative encoding (Golby et al., 2001, Kelley et al., 1998), and the right to spatial navigation and context-sensitive retrieval (Zheng et al., 2019). At a finer anatomical scale, Stevenson et al. identified a gradient along the hippocampal long axis, with left-lateralized pattern separation signals in anterior DG/CA3 and right-lateralized source memory signals in posterior CA1 and subiculum (Stevenson et al., 2020). Complementing these structural findings, Penner et al. (Penner et al., 2022) reported hemispheric differences in hippocampal theta bursts, including their frequency, amplitude, morphology, and prevalence, suggesting distinct mechanisms of theta generation across hemispheres. Our findings build on this work by demonstrating a functional asymmetry in how theta power relates to decision dynamics. These temporal effects suggest that hemispheric specialization in the hippocampus extends beyond static anatomical or domain-specific roles to include dynamic influences on how memory signals are integrated into decision-making in real time.

Despite hemispheric asymmetries in novelty- and familiarity-driven decisions, we also found that theta activity in both hippocampi enhanced drift toward correct "similar" responses during lure trials—those most indicative of pattern separation. This bilateral effect suggests that, under high mnemonic-perceptual ambiguity, both hemispheres jointly support evidence accumulation leading to accurate discrimination. This finding aligns with prior fMRI work demonstrating bilateral DG/CA3 engagement during lure discrimination in the MST (Reagh & Yassa, 2014), and supports the view that pattern separation is not strictly lateralized but can emerge from coordinated dynamics across hemispheres. Our results further suggest that this bilateral theta engagement is functionally complementary. In the left hemisphere, theta activity promotes novelty-sensitive discrimination, aiding the detection of subtle differences between lure stimuli and previously encoded memory traces. By emphasizing partial novelty, the left hippocampus reduces incorrect "old" responses and supports more nuanced judgments of similarity. In the right hemisphere, theta is associated with the suppression of generalized familiarity signals, effectively dampening inappropriate drift toward "old" responses. Thus, the right hippocampus contributes by ensuring a precise evaluation of stimulus familiarity, further reinforcing correct identification of lures as "similar." Together, these complementary hemispheric dynamics refine existing models of hippocampal function, revealing that successful pattern separation emerges from temporally coordinated novelty and familiarity processing across hemispheres.

Although hippocampal sources are challenging to resolve with MEG, our event-related fields (ERF) analysis demonstrates that temporally reliable, stimulus-locked activity can be detected from this deep brain structure. Group-averaged root-mean-square (RMS) time courses revealed a consistent response pattern in both hippocampi during both during both encoding and retrieval, characterized by an initial deflection beginning around 100 ms after stimulus onset, a polyphasic wave peaking between 200–300 ms, and a smaller subsequent peak between 400–500 ms. This temporal profile closely aligns with previous MEG findings of hippocampal activity during recognition memory tasks (Gonsalves et al., 2005, Riggs et al., 2009). The early onset of this response suggests that hippocampal contributions to recognition begin rapidly, potentially in parallel with visual processing (Riggs et al., 2009), while the later sustained component likely reflects ongoing mnemonic evaluation processes such as recollection (Gonsalves et al., 2005, Riggs et al., 2009). These results add to growing evidence that MEG, when combined with appropriate source modeling and localization methods, can reliably detect signals from deep brain structures such as the hippocampus (Bénar et al., 2021, López-Madrona et al., 2022, Pizzo et al., 2019). Although our RMS-based aggregation across dipoles precludes subfield-level analysis, it provides a robust estimate of hippocampal engagement suitable for assessing condition-related evoked dynamics.

While our findings underscore the utility of combining computational modeling with source-localized MEG, several methodological considerations warrant caution. First, although our sample size ($N = 15$) was sufficient to support robust within-subject modeling of neural and behavioral dynamics, the demographics may limit generalizability. The sample was predominantly female (14 of 15 participants), which may introduce bias given known sex differences in episodic memory and pattern separation (Herlitz et al., 1997, Yagi et al., 2016). Additionally, the cohort was relatively young (mean age 31), and age-related changes in hippocampal circuitry and pattern separation performance (Riphagen et al., 2020, Stark et al., 2013, Yassa & Stark, 2011) may constrain the applicability of these findings to older populations. Second, although recent work has validated the feasibility of localizing hippocampal sources with MEG, such estimates remain constrained by signal-to-noise ratios, inverse modeling assumptions, and anatomical variability. We employed conservative localization procedures based on individualized MRI models and constrained dynamic statistical parametric mapping (dSPM) estimates. Our interpretations remain at the level of whole hippocampal dynamics. Emerging techniques—such as reciprocal boundary element fast multipole method (BEM-FMM) (Drumm et al., 2025, Wartman et al., 2025)—offer promising avenues for improving spatial specificity in

future studies. Finally, while the LBA model offers a principled decomposition of decision processes, it necessarily abstracts over factors such as strategic shifts or attentional variability. Nevertheless, by linking trial-level neural activity to model-derived indices of evidence accumulation, our approach advances the integration of cognitive theory with temporally precise neurophysiological data.

Looking forward, this integrative framework opens new avenues for investigating the neural dynamics of memory-guided decision-making. Future work could extend these findings to populations with known impairments in hippocampal function—such as older adults, individuals with mild cognitive impairment, or those with affective disorders—in whom pattern separation deficits are well documented (Déry et al., 2013, Stark et al., 2013). Moreover, causal interventions targeting theta oscillations—via transcranial brain stimulation Deng et al. (2015), pharmacological modulation, or behavioral entrainment—could further elucidate the functional role of theta in biasing hippocampal computations. Finally, expanding this approach to other neural markers or brain regions may refine our understanding of how distributed circuits coordinate under conditions of uncertainty. By combining fine-grained behavioral modeling with temporally resolved neurophysiology, we move closer to a mechanistic account of how memory is transformed into decision.

5 | CONCLUSIONS

Our study demonstrates that hippocampal theta oscillations predict the rate of evidence accumulation during mnemonic decision-making. By combining source-localized magnetoencephalography (MEG) with linear ballistic accumulator (LBA) modeling, we show that trial-by-trial fluctuations in theta power predict decision quality in a computationally explicit manner. Crucially, these effects diverge across hemispheres: left hippocampal theta facilitates novelty-driven accumulation, while right hippocampal theta suppresses inappropriate familiarity, revealing a functionally complementary, push–pull mechanism. This temporally patterned asymmetry extends prior models of hippocampal function—often framed in structural or domain-level terms—by highlighting the dynamic contributions of each hemisphere to resolving mnemonic ambiguity. More broadly, our results underscore the utility of linking neural oscillations to latent decision parameters, offering a powerful framework for bridging cognitive theories of memory with their neural implementation. Finally, by demonstrating reliable hippocampal signal detection with MEG, this work affirms the feasibility of noninvasive deep-source modeling and sets the stage for future investigations of how brain rhythms govern cognition in real time.

AUTHOR CONTRIBUTIONS

Conceptualization, Z.-D.D. and P.L.R.; methodology, P.L.R., J.R.G., and Z.-D.D.; validation, P.L.R., J.D.S., F.W.C., and Z.-D.D.; formal analysis, P.L.R. and Z.-D.D.; data curation, J.R.G., N.M., P.L.R., and Z.-D.D.; writing–original draft preparation, P.L.R. and Z.-D.D.; writing–review and editing, P.L.R., J.R.G., B.L., N.M., E.B., J.D.S., F.W.C., and Z.-D.D.; visualization, P.L.R. and Z.-D.D.; supervision, Z.-D.D. All authors have read and agreed to the published version of the manuscript.

ACKNOWLEDGMENTS

Computational analyses were performed using the NIH HPC Biowulf cluster (http://hpc.nih.gov). The authors thank the NIMH MEG Core Facility for their contributions to data acquisition and technical support. We thank Alexandra Halberstadt for programming the mnemonic task in PsychoPy. The views expressed in this article are the author's own and do not reflect the views of the NIH, the Department of Health and Human Services, or the United States government.

CONFLICT OF INTEREST

The authors declare no conflicts of interest.

REFERENCES

Addante, R. J., Watrous, A. J., Yonelinas, A. P., Ekstrom, A. D., & Ranganath, C. (2011). Prestimulus theta activity predicts correct source memory retrieval. *Proc Natl Acad Sci U S A*, *108*(26), 10702–10707. doi: 10.1073/pnas.1014528108

Allegra, M., Posani, L., Gómez-Ocádiz, R., & Schmidt-Hieber, C. (2020). Differential relation between neuronal and behavioral discrimination during hippocampal memory encoding. *Neuron*, *108*(6), 1103–1112. doi: 10.1016/j.neuron.2020.09.032

Attal, Y., Bhattacharjee, M., Yelnik, J., Cottereau, B., Lefèvre, J., Okada, Y., ... Baillet, S. (2009). Modelling and detecting deep brain activity with MEG and EEG. *IRBM*, *30*(3), 133–138. doi: 10.1016/j.irbm.2009.01.005

Attal, Y., & Schwartz, D. (2013). Assessment of subcortical source localization using deep brain activity imaging model with minimum norm operators: A MEG study. *PLoS One*, *8*(3), e59856. doi: 10.1371/journal.pone.0059856

Bakker, A., Kirwan, C. B., Miller, M., & Stark, C. E. L. (2008). Pattern separation in the human hippocampal CA3 and dentate gyrus. *Science*, *319*(5870), 1640–1642. doi: 10.1126/science.1152882

Banavar, N. V., Noh, S. M., Wahlheim, C. N., Cassidy, B. S., Kirwan, C. B., Stark, C. E. L., & Bornstein, A. M. (2024). A response time model of the three-choice Mnemonic Similarity Task provides stable, mechanistically interpretable individual-difference measures. *Front Hum Neurosci*, *18*, 1379287. doi: 10.3389/fnhum.2024.1379287

Bénar, C.-G., Velmurugan, J., López-Madrona, V. J., Pizzo, F., & Badier, J.-M. (2021). Detection and localization of deep sources in magnetoencephalography: A review. *Curr Opin Biomed Eng*, *18*, 100285. doi: 10.1016/j.cobme.2021.100285

Berron, D., Schütze, H., Maass, A., Cardenas-Blanco, A., Kuijf, H. J., Kumaran, D., & Düzel, E. (2016). Strong evidence for pattern separation in human dentate gyrus. *Journal of Neuroscience*, *36*(29), 7569–7579. doi: 10.1523/JNEUROSCI.0518-16.2016

Brown, S. D., & Heathcote, A. (2008). The simplest complete model of choice response time: Linear ballistic accumulation. *Cogn Psychol*, *57*(3), 153–178. doi: 10.1016/j.cogpsych.2007.12.002

Buzsáki, G. (2002). Theta oscillations in the hippocampus. *Neuron*, *33*(3), 325–340. doi: 10.1016/s0896-6273(02)00586-x

Carpenter, B., Gelman, A., Hoffman, M. D., Lee, D., Goodrich, B., Betancourt, M., … Riddell, A. (2017). Stan: A probabilistic programming language. *J Stat Softw*, *76*(1), 1–32. doi: 10.18637/jss.v076.i01

Colgin, L. L. (2013). Mechanisms and functions of theta rhythms. *Annu Rev Neurosci*, *36*, 295–312. doi: 10.1146/annurev-neuro-062012-170330

Dale, A. M., Liu, A. K., Fischl, B. R., Buckner, R. L., Belliveau, J. W., Lewine, J. D., & Halgren, E. (2000). Dynamic statistical parametric mapping: combining fMRI and MEG for high-resolution imaging of cortical activity. *Neuron*, *26*(1), 55–67. doi: 10.1016/s0896-6273(00)81138-1

Deng, Z.-D., McClintock, S. M., Oey, N. E., Luber, B., & Lisanby, S. H. (2015). Neuromodulation for mood and memory: from the engineering bench to the patient bedside. *Curr Opin Neurobiol*, *30*, 38–43. doi: 10.1016/j.conb.2014.08.015

Déry, N., Pilgrim, M., Gibala, M., Gillen, J., Wojtowicz, J. M., MacQueen, G., & Becker, S. (2013). Adult hippocampal neurogenesis reduces memory interference in humans: Opposing effects of aerobic exercise and depression. *Front Neurosci*, *7*, 66. doi: 10.3389/fnins.2013.00066

Donkin, C., Brown, S., Heathcote, A., & Wagenmakers, E.-J. (2011). Diffusion versus linear ballistic accumulation: Different models but the same conclusions about psychological processes? *Psychon Bull Rev*, *18*(1), 61–69. doi: 10.3758/s13423-010-0022-4

Drumm, D. A., Nuñez Ponasso, G., Linke, A., Noetscher, G. M., Maess, B., Knösche, T. R., … Deng, Z.-D. (2025). Improved source localization of auditory evoked fields using reciprocal BEM-FMM. *bioRxiv*. doi: 10.1101/2025.05.09.653081

Eichenbaum, H. (2017). Prefrontal–hippocampal interactions in episodic memory. *Nat Rev Neurosci*, *18*(9), 547–558. doi: 10.1038/nrn.2017.74

Fell, J., Ludowig, E., Staresina, B. P., Wagner, T., Kranz, T., Elger, C. E., & Axmacher, N. (2011). Medial temporal theta/alpha power enhancement precedes successful memory encoding: Evidence from intracranial EEG. *J Neurosci*, *31*(14), 5392–5397. doi: 10.1523/JNEUROSCI.3668-10.2011

Fischl, B. (2013). FreeSurfer. *Neuroimage*, *62*(2), 774–781. doi: 10.1016/j.neuroimage.2012.01.021

Golby, A. J., Poldrack, R. A., Brewer, J. B., Spencer, D., Desmond, J. E., Aron, A. P., & Gabrieli, J. D. (2001). Material-specific lateralization in the medial temporal lobe and prefrontal cortex during memory encoding. *Brain*, *124*(9), 1841–1854. doi: 10.1093/brain/124.9.1841

Gonsalves, B. D., Kahn, I., Curran, T., Norman, K. A., & Wagner, A. D. (2005). Memory strength and repetition suppression: Multimodal imaging of medial temporal cortical contributions to recognition. *Neuron*, *47*(5), 751–761. doi: 10.1016/j.neuron.2005.07.013

Guderian, S., Schott, B. H., Richardson-Klavehn, A., & Düzel. (2009). Medial temporal theta state before an event predictsepisodic encoding success in humans. *Proc Natl Acad Sci U S A*, *106*(13), 5365–5370. doi: 10.1073/pnas.0900289106

Hasselmo, M. E. (2005). What is the function of hippocampal theta rhythm?–Linking behavioral data to phasic properties of field potential and unit recording data. *Hippocampus*, *15*(7), 936–949. doi: 10.1002/hipo.20116

Hasselmo, M. E., Bodelón, C., & Wyble, B. P. (2002). A proposed function for hippocampal theta rhythm: Separate phases of encoding and retrieval enhance reversal of prior learning. *Neural Comput*, *14*(4), 793–817. doi: 10.1162/089976602317318965

Herlitz, A., Nilsson, L.-G., & Bäckman, L. (1997). Gender differences in episodic memory. *Mem Cognit*, *25*(6), 801–811. doi: 10.3758/bf03211324

Herweg, N. A., Solomon, E. A., & Kahana, M. J. (2020). Theta oscillations in human memory. *Trends Cogn Sci*, *24*(3), 208–227. doi: 10.1016/j.tics.2019.12.006

Kelley, W. M., Miezin, F. M., McDermott, K. B., Buckner, R. L., Raichle, M. E., Cohen, N. J., … Petersen, S. E. (1998). Hemispheric specialization in human dorsal frontal cortex and medial temporal lobe for verbal and nonverbal memory encoding. *Neuron*, *20*(5), 927–936. doi: 10.1016/s0896-6273(00)80474-2

Leutgeb, J. K., Leutgeb, S., Moser, M.-B., & Moser, E. I. (2007). Pattern separation in the dentate gyrus and CA3 of the hippocampus. *Science*, *315*(5814), 961–966. doi: 10.1126/science.1135801

López-Madrona, V. J., Medina Villalon, S., Badier, J. M., Tréuchon, A., Jayabal, V., Bartolomei, F., … Bénar, C. G. (2022). Magnetoencephalography can reveal deep brain network activities linked to memory processes. *Hum Brain Mapp*, *43*(15), 4733–4749. doi: 10.1002/hbm.25987

Mueller, C. J., White, C. N., & Kuchinke, L. (2017). Electrophysiological correlates of the drift diffusion model in visual word recognition. *Hum Brain Mapp*, *38*(11), 5616–5627. doi: 10.1002/hbm.23753

Mulder, M. J., van Maanen, L., & Forstmann, B. U. (2014). Perceptual decision neurosciences - a model-based review. *Neuroscience*, *277*, 872–884. doi: 10.1016/j.neuroscience.2014.07.031

O'Reilly, R. C., & McClelland, J. L. (1994). Hippocampal conjunctive encoding, storage, and recall: Avoiding a trade-off. *Hippocampus*, *4*(5), 661–682. doi: 10.1002/hipo.450040605

Osipova, D., Takashima, A., Oostenveld, R., Fernández, G., Maris, E., & Jensen, O. (2006). Theta and gamma oscillations predict encoding and retrieval of declarative memory. *J Neurosci*, *26*(28), 7523–7531. doi: 10.1523/JNEUROSCI.1948-06.2006

Peirce, J., Gray, J. R., Simpson, S., MacAskill, M., Höchenberger, R., Sogo, H., … Lindeløv, J. K. (2019). PsychoPy2: Experiments in behavior made easy. *Behav Res Methods*, *51*(1), 195–203. doi: 10.3758/s13428-018-01193-y

Penner, C., Minxha, J., Chandravadia, N., Mamelak, A. N., & Rutishauser, U. (2022). Properties and hemispheric differences of theta oscillations inthe human hippocampus. *Hippocampus*, *32*(5), 335–341. doi: 10.1002/hipo.23412

Philiastides, M. G., & Sajda, P. (2006). Temporal characterization of the neural correlates of perceptual decision making in the human brain. *Cereb Cortex*, *16*(4), 509–518. doi: 10.1093/cercor/bhi130

Pizzo, F., Roehri, N., Medina Villalon, S., Tréuchon, A., Chen, S., Lagarde, S., … Bénar, C. G. (2019). Deep brain activities can be detected with magnetoencephalography. *Nat Commun*, *10*, 971. doi: 10.1038/s41467-019-08665-5

Ratcliff, R., Philiastides, M. G., & Sajda, P. (2009). Quality of evidence for perceptual decision making is indexed by trial-to-trial variability of the EEG. *Proc Natl Acad Sci U S A*, *106*(16), 6539–6544. doi: 10.1073/pnas.0812589106

Reagh, Z. M., & Yassa, M. A. (2014). Object and spatial mnemonic interference differentially engage lateral and medial entorhinal cortex in humans. *Proc Natl Acad Sci U S A*, *111*(40), E4264–E4273. doi: 10.1073/pnas.1411250111

Riggs, L., Moses, S. N., Bardouille, T., Herdman, A. T., Ross, B., & Ryan, J. D. (2009). A complementary analytic approach to examining medial temporal lobe sourcesusing magnetoencephalography. *Neuroimage*, *45*(2), 627–642. doi: 10.1016/j.neuroimage.2008.11.018

Riphagen, J. M., Schmiedek, L., Gronenschild, E. H. B. M., Yassa, M. A., Priovoulos, N., Sack, A. T., … Jacobs, H. I. L. (2020). Associations between pattern separation and hippocampal subfield structure and function vary along the lifespan: A 7 T imaging study. *Sci Rep*, *10*(1), 7572. doi: 10.1038/s41598-020-64595-z

Rolls, E. T. (2013). The mechanisms for pattern completion and pattern separation in the hippocampus. *Front Syst Neurosci*, *7*, 74. doi: 10.3389/fnsys.2013.00074

Stan Development Team. (2024). *RStan: The R interface to Stan*. Retrieved from `https://mc-stan.org/` R package version 2.26.24.

Stark, S. M., Kirwan, C. B., & Stark, C. E. L. (2019). Mnemonic similarity task: A tool for assessing hippocampal integrity. *Trends Cogn Sci*, *23*(11), 938–951. doi: 10.1016/j.tics.2019.08.003

Stark, S. M., Yassa, M. A., Lacy, J. W., & Stark, C. E. L. (2013). A task to assess behavioral pattern separation (BPS) in humans: Data from healthy aging and mild cognitive impairment. *Neuropsychologia*, *51*(12), 2442–2449. doi: 10.1016/j.neuropsychologia.2012.12.014

Stevenson, R. F., Reagh, Z. M., Chun, A. P., Murray, E. A., & Yassa, M. A. (2020). Pattern separation and source memory engage distinct hippocampal and neocortical regions during retrieval. *J Neurosci*, *40*(4), 843–851. doi: 10.1523/JNEUROSCI.0564-19.2019

Tadel, F., Baillet, S., Mosher, J. C., Pantazis, D., & Leahy, R. M. (2011). Brainstorm: A user-friendly application for MEG/EEG analysis. *Comput Intell Neurosci*, *2011*, 879716. doi: 10.1155/2011/879716

Treves, A., & Rolls, E. T. (1994). Computational analysis of the role of the hippocampus in memory. *Hippocampus*, *4*(3), 374–391. doi: 10.1002/hipo.450040319

Tulving, E. (1983). *Elements of Episodic Memory*. Oxford, UK: Oxford University Press.

Tulving, E., Kapur, S., Craik, F. I., Moscovitch, M., & Houle, S. (1994). Hemispheric encoding/retrieval asymmetry in episodic memory: Positron emission tomography findings. *Proc Natl Acad Sci U S A*, *91*(6), 2016–2020. doi: 10.1073/pnas.91.6.2016

Vehtari, A., Gelman, A., Simpson, D., Carpenter, B., & Bürkner, P.-C. (2021). Rank-normalization, folding, and localization: An improved $\hat{R}$ for assessing convergence of MCMC (with discussion). *Bayesian Anal*, *16*(2), 667–718. doi: 10.1214/20-BA1221

Wartman, W. A., Nuñez Ponasso, G., Qi, Z., Haueisen, J., Maess, B., Knösche, T. R., … Makaroff, S. N. (2025). Fast EEG/MEG BEM-based forward problem solution for high-resolution head models. *Neuroimage*, *306*, 120998. doi: 10.1016/j.neuroimage.2024.120998

Yagi, S., Chow, C., Lieblich, S. E., & Galea, L. A. M. (2016). Sex and strategy use matters for pattern separation, adult neurogenesis, and immediate early gene expression in the hippocampus. *Hippocampus*, *26*(1), 87–101. doi: 10.1002/hipo.22493

Yassa, M. A., & Stark, C. E. L. (2011). Pattern separation in the hippocampus. *Trends Neurosci*, *34*(10), 515–525. doi: 10.1016/j.tins.2011.06.006

Yassa, M. A., Stark, S. M., Bakker, A., Albert, M. S., Gallagher, M., & Stark, C. E. L. (2011). High-resolution structural and functional MRI of hippocampal CA3 and dentate gyrus in patients with amnestic mild cognitive impairment. *Neuroimage*, *51*(3), 1242–1252. doi: 10.1016/j.neuroimage.2010.03.040

Zheng, J., Stevenson, R. F., Mander, B. A., Mnatsakanyan, L., Hsu, F. P. K., Vadera, S., … Lin, J. J. (2019). Multiplexing of theta and alpha rhythms in the amygdala-hippocampal circuit supports pattern separation of emotional information. *Neuron*, *102*(4), 887–898. doi: 10.1016/j.neuron.2019.03.025